THE JOURNAL OF BIOLOGICAL CHEMISTRY VOL. 291, NO. 36, pp. 19031–19041, September 2, 2016
Published in the U.S.A.

An Oral Load of [$^{13}C_3$]Glycerol and Blood NMR Analysis Detect Fatty Acid Esterification, Pentose Phosphate Pathway, and Glycerol Metabolism through the Tricarboxylic Acid Cycle in Human Liver*

Received for publication, June 7, 2016, and in revised form, July 15, 2016 Published, JBC Papers in Press, July 18, 2016, DOI 10.1074/jbc.M116.742262

Eunsook S. Jin[‡§1], **A. Dean Sherry**[‡¶‖], **and Craig R. Malloy**[‡§¶**]

From the [‡]*Advanced Imaging Research Center and the Departments of* [§]*Internal Medicine and* [¶]*Radiology, University of Texas Southwestern Medical Center at Dallas, Dallas, Texas 75390, the* [‖]*Department of Chemistry, University of Texas at Dallas, Richardson, Texas 75080, and the* **VA North Texas Health Care System, Dallas, Texas 75216*

Drugs and other interventions for high impact hepatic diseases often target biochemical pathways such as gluconeogenesis, lipogenesis, or the metabolic response to oxidative stress. However, traditional liver function tests do not provide quantitative data about these pathways. In this study, we developed a simple method to evaluate these processes by NMR analysis of plasma metabolites. Healthy subjects ingested [U-$^{13}C_3$]glycerol, and blood was drawn at multiple times. Each subject completed three visits under differing nutritional states. High resolution ^{13}C NMR spectra of plasma triacylglycerols and glucose provided new insights into a number of hepatic processes including fatty acid esterification, the pentose phosphate pathway, and gluconeogenesis through the tricarboxylic acid cycle. Fasting stimulated pentose phosphate pathway activity and metabolism of [U-$^{13}C_3$]glycerol in the tricarboxylic acid cycle prior to gluconeogenesis or glyceroneogenesis. Fatty acid esterification was transient in the fasted state but continuous under fed conditions. We conclude that a simple NMR analysis of blood metabolites provides an important biomarker of pentose phosphate pathway activity, triacylglycerol synthesis, and flux through anaplerotic pathways in mitochondria of human liver.

Clinical evaluation of liver function involves measurement of circulating clotting factors and other proteins, transaminases, and bilirubin. Although these assays are essential for patient management, traditional "liver function tests" are not specific for the metabolic pathways that underlie high impact disorders. Many liver diseases are associated with abnormal mitochondrial function or impaired defense against oxidative stress, and drugs specifically designed to reduce oxidative injury (1, 2), inhibit hepatic triacylglycerol (TAG)[2] synthesis (3, 4), or block gluconeogenesis via the TCA cycle (5, 6) are widely prescribed. Nevertheless it is difficult to probe activity of the TCA cycle, the pentose phosphate pathway (PPP) or fatty acid esterification in human subjects. A liver biopsy provides valuable information, but biopsies are constrained by sampling errors, morbidity, and mortality (7). Administration of substrates labeled with stable isotopes followed by analysis of plasma metabolites is a powerful approach for assessing gluconeogenesis and lipogenesis in the human liver. However, these methods typically involve intravenous administration of isotopes (8–12) or multiple NMR measurements with the subject in a magnet (13, 14). Technical requirements limit general utility.

Recently methods were introduced to study hepatic PPP by analysis of plasma glucose and hepatic fatty acid esterification in rodents receiving intragastric ^{13}C-labeled glycerol (15, 16). After the administration of [U-$^{13}C_3$]glycerol, different metabolic pathways in the liver generate unique ^{13}C-labeling patterns in the products of hepatic biosynthesis, glucose and TAGs, that are exported into circulation and readily sampled in venous blood. The ^{13}C-labeling patterns provide a rich source of information regarding multiple pathways including fatty acid esterification, gluconeogenesis, the PPP, and TCA cycle activity. Direct conversion of [U-$^{13}C_3$]glycerol to either glucose or TAGs retains the intact ^{13}C-unit of three covalently bonded carbons (^{13}C-^{13}C-^{13}C) of the original glycerol. Metabolism of [U-$^{13}C_3$]glycerol in the TCA cycle followed by resynthesis to a triose during gluconeogenesis yields a double-labeled (^{13}C-^{13}C) triose. Thus, the detection of glucose or glycerol derived from a double-labeled triose indicates metabolism of [U-$^{13}C_3$]glycerol through the TCA cycle prior to formation of these products. In addition, the difference in labeling patterns between glucose carbons 1–3 *versus* carbons 4–6 after the administration of [U-$^{13}C_3$]glycerol provides an index of hepatic PPP activity. The oxidative arm of the PPP rearranges carbons 1–3 but not carbons 4–6. The details of these pathways are illustrated in Fig. 1.

Here we investigated the metabolism of [U-$^{13}C_3$]glycerol in human subjects to test the hypothesis that a portion of glycerol is metabolized in the TCA cycle prior to glyceroneogenesis or gluconeogenesis. Healthy volunteers ingested [U-$^{13}C_3$]glycerol under differing nutritional states. Blood was drawn at multiple times, and metabolites from blood were analyzed using ^{13}C NMR. In addition to fasted and fed conditions, we evaluated the

* This work was supported by National Institutes of Health Grants DK099289 (to E. S. J.), DK058398 and EB015908 (to C. R. M.), and HL34557 (to A. D. S.). The authors declare that they have no conflicts of interest with the contents of this article. The content is solely the responsibility of the authors and does not necessarily represent the official views of the National Institutes of Health.

[1] To whom correspondence should be addressed: Advanced Imaging Research Center, 5323 Harry Hines Blvd., Dallas, TX 75390-8568. Tel.: 214-645-2725; Fax: 214-645-2744; E-mail: eunsook.jin@utsouthwestern.edu.

[2] The abbreviations used are: TAG, triacylglycerol; DHAP, dihydroxyacetone phosphate; GA3P, D-glyceraldehyde 3-phosphate; PEP, phospho*enol*pyruvate; PPP, pentose phosphate pathway.

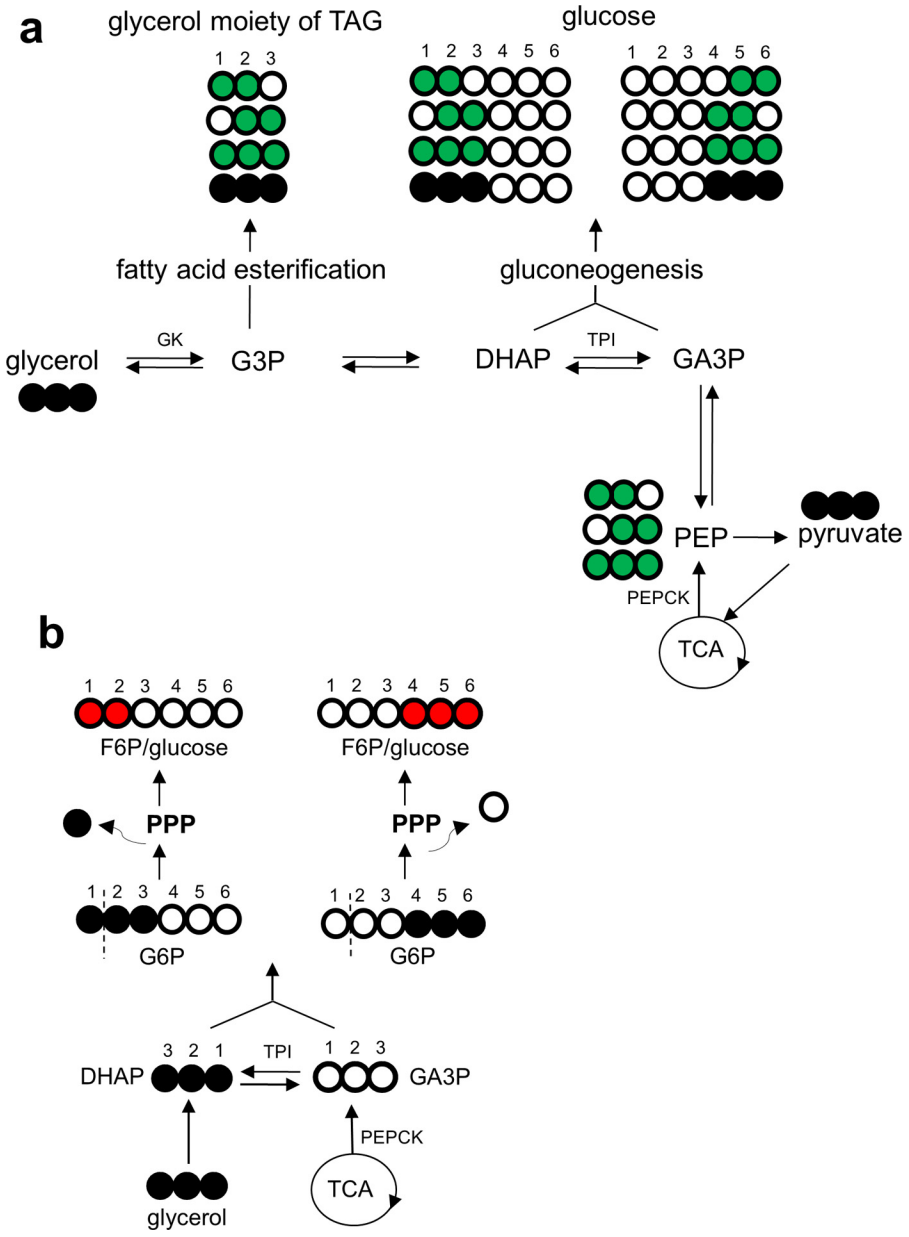

FIGURE 1. **^{13}C labeling patterns in TAGs and glucose produced in liver after oral [U-$^{13}C_3$]glycerol.** *a*, [U-$^{13}C_3$]glycerol may be used immediately as backbones for fatty acid esterification or in gluconeogenesis after phosphorylation ("direct" contribution). A fraction of [U-$^{13}C_3$]glycerol may be further converted to other trioses and [U-$^{13}C_3$]pyruvate entering the TCA cycle prior to glyceroneogenesis or gluconeogenesis ("indirect" contribution). The TCA cycle scrambles ^{13}C extensively, labeling all the cycle intermediates, including oxaloacetate, that may exit the cycle producing double- or triple-labeled trioses. These trioses may be either glyceroneogenic or gluconeogenic. Because PEP is a common intermediate for DHAP (becoming glucose carbons 1–3) and GA3P (becoming glucose carbons 4–6), an equivalent ^{13}C-labeling pattern is expected between glucose carbons 1–3 and carbons 4–6. Thus, the ratio [1,2-$^{13}C_2$]/[2,3-$^{13}C_2$] in glucose must be equal to the ratio [5,6-$^{13}C_2$]/[4,5-$^{13}C_2$] in glucose. *b*, however, PPP activity increases the ratio of [1,2-$^{13}C_2$]/[2,3-$^{13}C_2$], but not [5,6-$^{13}C_2$]/[4,5-$^{13}C_2$], by producing [1,2-$^{13}C_2$]hexose. Gluconeogenesis directly from [U-$^{13}C_3$]glycerol produces [1,2,3-$^{13}C_3$]- or [4,5,6-$^{13}C_3$]hexose. The entry of [1,2,3-$^{13}C_3$]glucose 6-phosphate to PPP produces mainly [1,2-$^{13}C_2$]fructose 6-phosphate through decarboxylation in the oxidative PPP followed by carbon rearrangement in the non-oxidative PPP. In contrast, ^{13}C 3-unit (^{13}C-^{13}C-^{13}C) in [4,5,6-$^{13}C_3$]hexose remains the same even after passing through the PPP. Consequently, the ^{13}C-labeling pattern in glucose carbons 1–3 is sensitive to PPP activity, but the pattern in glucose carbons 4–6 is not. *Open circles*, ^{12}C; *black circles*, ^{13}C; *green circles*, ^{13}C after metabolism through the TCA cycle; *red circles*, ^{13}C after metabolism through the PPP. F6P, fructose 6-phosphate; G3P, glycerol 3-phosphate; G6P, glucose 6-phosphate; GK, glycerol kinase; *PEPCK*, PEP carboxykinase; *TPI*, triose phosphate isomerase.

consequences of a bolus of oral glucose (here termed "fed plus glucose") to determine whether a high concentration of glucose would stimulate hepatic PPP to supply NADPH needed for fatty acid synthesis. Although the majority of the carbon backbones of TAGs was directly derived from [U-$^{13}C_3$]glycerol, ~5–20% was derived after metabolism of glycerol in the TCA cycle. Glycerol metabolism in the TCA cycle and PPP activity were both more active in the fasted state compared with the fed states. Key metabolic processes in the liver of human subjects including glycerol metabolism in the TCA cycle, the PPP, and fatty acid esterification were sensitive to nutritional states, and these processes were detected using a protocol that requires only oral administration of glycerol and venous blood samples. This assay is convenient and acceptable to human subjects, and in a single exam it detects metabolic pathways in the liver that were previously inaccessible in a simple assay.

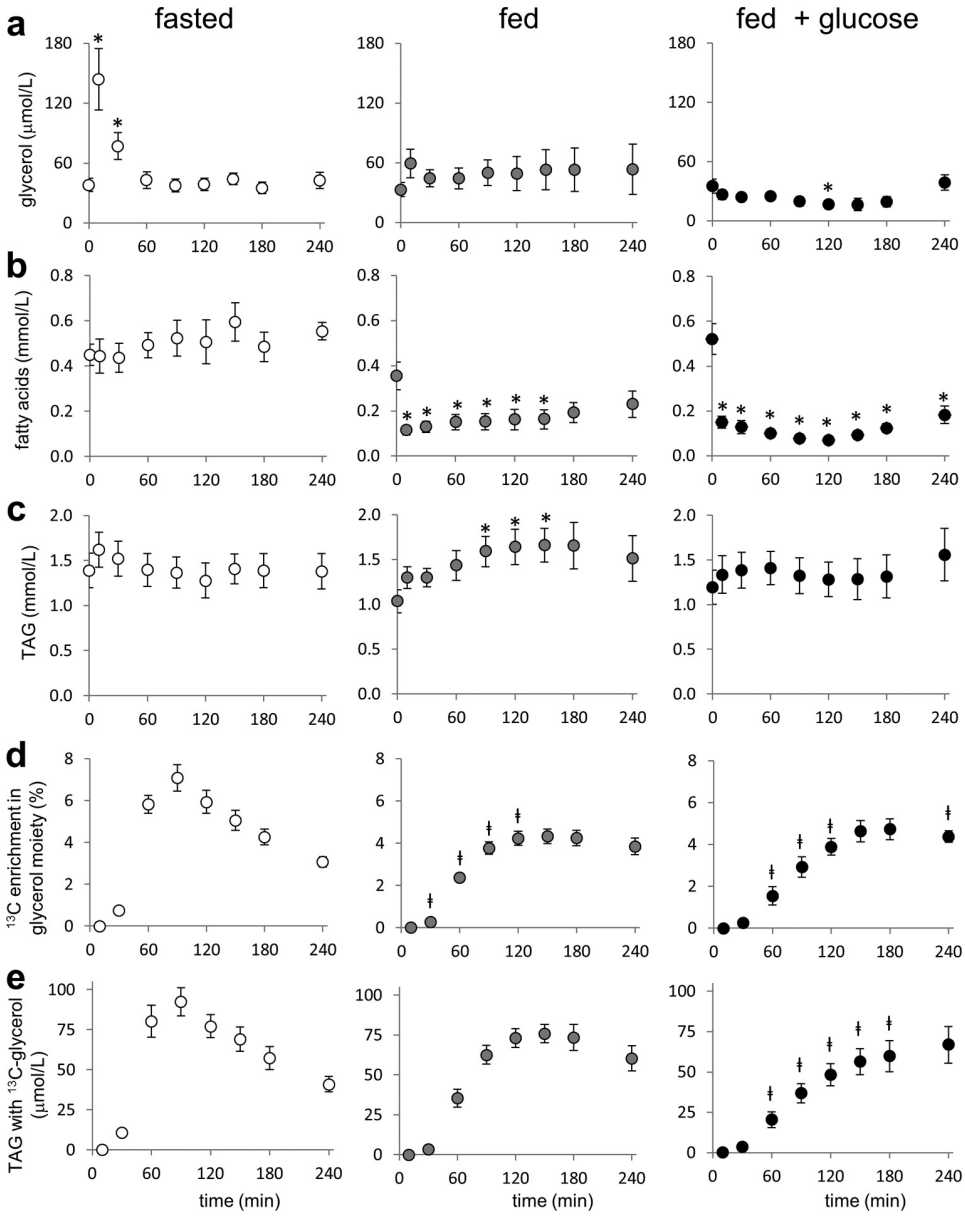

FIGURE 2. **Glycerol, fatty acids, TAGs, and ^{13}C incorporation to TAGs in plasma from subjects receiving [U-$^{13}C_3$]glycerol.** *a*, the concentration of free glycerol in plasma increased immediately after [U-$^{13}C_3$]glycerol ingestion under a fast but remained constant under fed conditions. *b*, the concentration of fatty acids was high under a fast but decreased by food intake. *c*, the concentration of TAGs was not significantly changed under a fasted state and a fed plus glucose condition but was higher at 90–150 min after [U-$^{13}C_3$]glycerol ingestion under a fed condition compared with the level after a fast ($t = 0$). *d*, after a fast, [U-$^{13}C_3$]glycerol ingestion led to rapid ^{13}C enrichment in the glycerol moiety and reached a maximum at 90 min. Under fed conditions, the fractional enrichment increased gradually reaching a plateau at ~150 min. *e*, the concentration of TAGs with excess ^{13}C-labeled glycerol backbones (*i.e.* newly synthesized TAGs) was greatest at 90 min under a fast and at 150 min under a fed state but steadily increased up to 240 min under a fed plus glucose condition. In each graph, the value at the zero time point ($t = 0$) was from an overnight fast prior to the administration of [U-$^{13}C_3$]glycerol, meal, or glucose. *, $p < 0.05$ compared with $t = 0$ in each graph; ‡, $p < 0.05$ compared with the corresponding time point under a fasted state ($n = 5–6$).

Results

Fasting Stimulates Metabolism of Glycerol in the TCA Cycle—The effects of nutritional states on the concentrations of plasma glycerol, fatty acids, and TAGs are shown in Fig. 2 (*a*–*c*). The ^{13}C NMR spectra of plasma metabolites were sensitive to nutritional states. Under all conditions, the^{13}C NMR spectra of plasma lipids showed well resolved resonances of the glycerol moiety of TAGs (Fig. 3*a*). The singlet (S) from carbon 1 (C1) and C3 resonance at 62.2 ppm reflects signals from single-labeled ([1-$^{13}C_1$] and [3-$^{13}C_1$]) glycerol, whereas the doublet (D) reflects contributions from double- and triple-labeled ([1,2-$^{13}C_2$], [2,3-$^{13}C_2$], and [U-$^{13}C_3$]) glycerol moieties. Given the low probability of forming a single-labeled glycerol moiety from exogenous [U-$^{13}C_3$]glycerol, the singlet was assumed to represent natural abundance ^{13}C (1.1%). The time course of ^{13}C enrichment in the glycerol backbones of TAGs was sensitive to nutritional states. Under a fast, ^{13}C enrichment in the glycerol backbones rapidly increased, reaching a maximum (7.1%) at 90 min after [U-$^{13}C_3$]glycerol ingestion, followed by gradual decrease. Under the fed or the fed plus glucose condition, the enrichment gradually increased, reaching a plateau at 120–150 min. (Fig. 2*d*). The concentration of TAGs with excess ^{13}C-

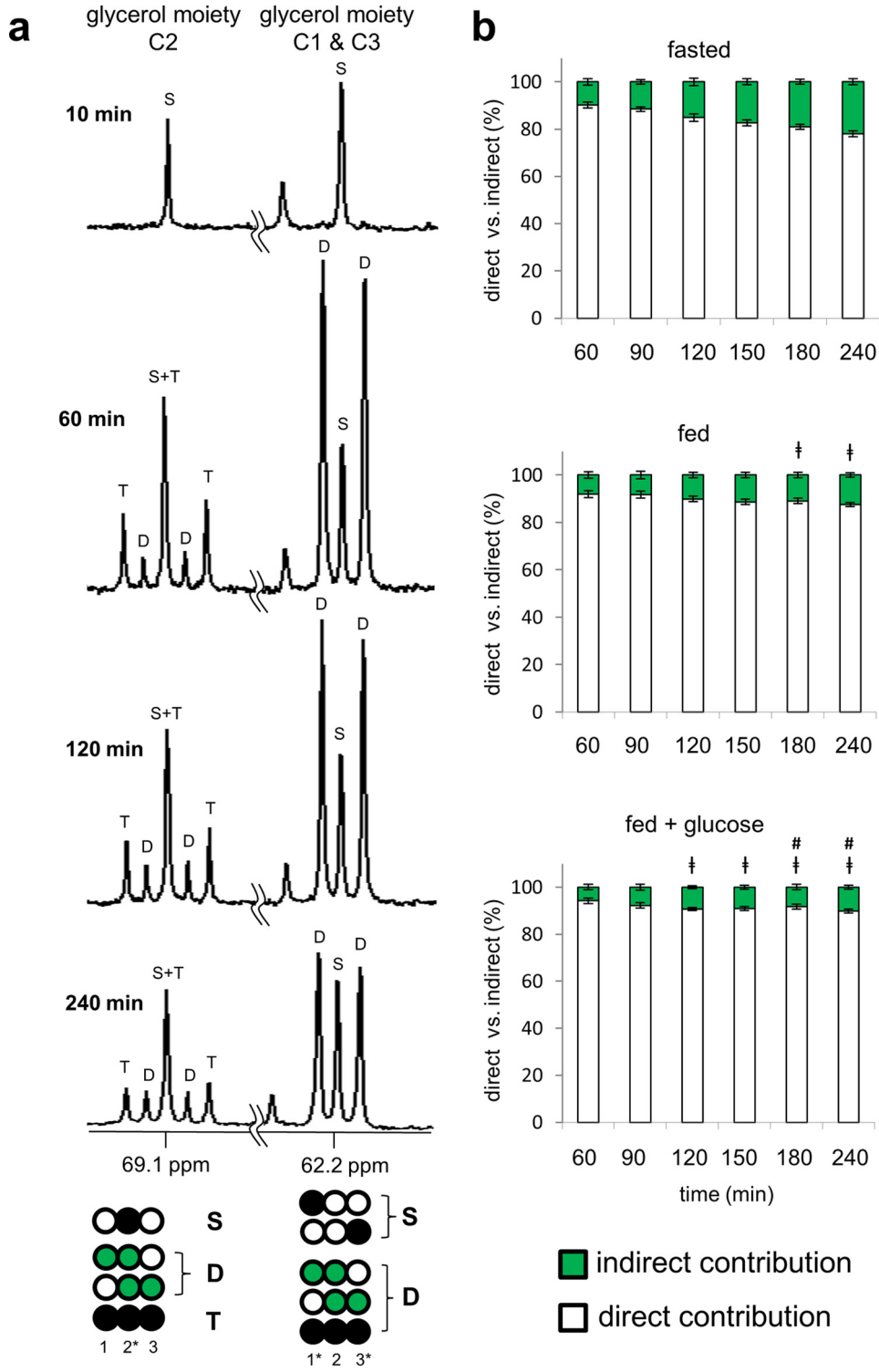

FIGURE 3. **^{13}C NMR spectra of the glycerol moiety of TAGs reflect direct and indirect contributions from [U-$^{13}C_3$]glycerol.** Healthy subjects ingested [U-$^{13}C_3$]glycerol under differing nutritional states, and blood was drawn at multiple times. *a*, ^{13}C NMR spectra of lipid extracts from a fasted subject show the resonances of the glycerol backbones of TAGs. The spectrum from 10 min shows natural abundance ^{13}C only, but the spectra from 60, 120, and 240 min show signals from excess ^{13}C in the glycerol backbones. In the C1 and C3 region at 62.2 ppm, the doublet (*D*) reflects signals from [1,2-$^{13}C_2$]-, [2,3-$^{13}C_2$]-, and [U-$^{13}C_3$]glycerol moieties of TAGs. In the C2 region at 69.1 ppm, the doublet (*D*) reflects [1,2-$^{13}C_2$]- and [2,3-$^{13}C_2$]glycerol moieties, and the triplet (*T*) arises exclusively from [U-$^{13}C_3$]glycerol moiety. The presence of double-labeled glycerol demonstrates metabolism of [U-$^{13}C_3$]glycerol in the TCA cycle prior to glyceroneogenesis. *b*, the direct *versus* indirect contribution from [U-$^{13}C_3$]glycerol was estimated based on the analysis of the glycerol moiety C2 resonance. [U-$^{13}C_3$]Glycerol incorporation to TAGs occurred primarily via the direct pathway under all nutritional conditions. The indirect contribution through the TCA cycle was minor but increased gradually over time and was sensitive to nutritional states. The indirect contribution was 22% after a fast, 13% under a fed condition, and 10% under a fed plus glucose condition at 240 min of the ingestion. *D*, doublet from coupling of C1 with C2 or from coupling of C2 with C3; *T*, triplet arising from coupling of C2 with both C1 and C3; *S*, singlet. *Open circles*, ^{12}C; *black circles*, ^{13}C; *green circles*, ^{13}C after metabolism through the TCA cycle. ‡, $p < 0.05$ compared with the corresponding time point under a fasted state; $^{\#}$, $p < 0.05$ compared with the corresponding time point under a fed state ($n = 6$).

labeled glycerol moiety indicates newly synthesized TAGs from the liver exported into the circulation and was calculated by multiplying [TAG] and the fraction of glycerol moiety with excess ^{13}C (Fig. 2*e*). The maximum concentration occurred early under both the fasted and fed states, but it steadily increased up to 240 min under the fed plus glucose condition.

The C2 resonance of the glycerol moiety at 69.1 ppm is composed of a natural abundance singlet, a doublet caused by either [1,2-$^{13}C_2$]glycerol or [2,3-$^{13}C_2$]glycerol or a 1:2:1 triplet caused by [U-$^{13}C_3$]glycerol (Fig. 3*a*). As noted, [U-$^{13}C_3$]glycerol metabolism directly to TAGs only produces an intact triple-labeled unit (^{13}C-^{13}C-^{13}C), yet double-labeled units (^{13}C-^{13}C) are also produced through the TCA cycle prior to glyceroneogenesis. Thus, any signal arising from the doublet must reflect the indirect contribution of [U-$^{13}C_3$]glycerol to TAGs after metabolism in the TCA cycle. The indirect contribution increased over time under all nutritional states but was ~2-fold greater after a fast. At 240 min after [U-$^{13}C_3$]glycerol ingestion, the indirect contribution was 22% in the fasting state, 13% in the fed state, and 10% in the fed plus glucose state (Fig. 3*b*). The indirect contributions at 10 and 30 min were not measured because of low ^{13}C enrichments.

Fasting Simulates PPP Activity and Gluconeogenesis from Glycerol—The concentration of plasma glucose remained constant after [U-$^{13}C_3$]glycerol ingestion in both the fasted and fed conditions but increased in the fed plus glucose condition at 10–60 min (Fig. 4*a*). In ^{13}C NMR spectra of monoacetone glucose derived from plasma glucose, signals from [1,2,3-$^{13}C_3$]- and [4,5,6-$^{13}C_3$]glucose were dominant under all nutritional states, reflecting gluconeogenesis directly from [U-$^{13}C_3$]glycerol (Fig. 5). The presence of double-labeled ([1,2-$^{13}C_2$], [2,3-$^{13}C_2$], [4,5-$^{13}C_2$], and [5,6-$^{13}C_2$]) glucose isotopomers demonstrates the metabolism of [U-$^{13}C_3$]glycerol through the TCA cycle prior to gluconeogenesis and is consistent with the observation in the glycerol backbones of TAGs. The sum of all glucose isotopomers with excess ^{13}C, indicating gluconeogenesis from [U-$^{13}C_3$]glycerol, was much higher after a fast compared with fed or fed plus glucose conditions (Fig. 4*b*). The difference between [1,2-$^{13}C_2$]/[2,3-$^{13}C_2$] and [5,6-$^{13}C_2$]/[4,5-$^{13}C_2$] ratios in glucose (reflecting PPP activity) was higher in the fasting than in the fed conditions (Fig. 4*c*). The amount of [1,2-$^{13}C_2$]glucose produced through the PPP, on the order of 1–40 μmol/liter, was much higher after a fast compared with the fed states (Fig. 4*d*). Nonetheless, the fraction of [1,2-$^{13}C_2$]glucose from the PPP was still less than 1% of plasma glucose pool even under fasting. When the PPP flux was compared with gluconeogenesis from [U-$^{13}C_3$]glycerol, it was ~5–6% after a fast and ~3% under fed states (Table 1).

Metabolism of [U-$^{13}C_3$]glycerol through the TCA cycle is reflected as doublets because of [1,2-$^{13}C_2$]glucose, [2,3-$^{13}C_2$]glucose, [4,5-$^{13}C_2$]glucose, and [5,6-$^{13}C_2$]glucose. Because [1,2-$^{13}C_2$]glucose and [2,3-$^{13}C_2$]glucose are sensitive to flux through the PPP, [5,6-$^{13}C_2$]glucose is a useful marker for metabolism of [U-$^{13}C_3$]glycerol through the TCA cycle because the signal from [4,5-$^{13}C_2$]glucose is small (Fig. 5). The fraction of [5,6-$^{13}C_2$]glucose in plasma glucose was much higher after a fast than fed states. The minimal [5,6-$^{13}C_2$]glucose production under the fed plus glucose condition was presumably due to suppression of gluconeogenesis by the glucose load in these healthy subjects (Fig. 4*e*).

Discussion

This study demonstrated that [U-$^{13}C_3$]glycerol is a useful and convenient probe of multiple key metabolic processes in the liver of human subjects. The utility arises from the combined features of negligible toxicity, ease of oral administration, the ability to access *de novo* synthesis of both glucose and TAGs under various nutritional states, and the abundant information yield arising from ^{13}C-^{13}C spin-spin couplings of the metabolic products in plasma. We demonstrated that the fraction of plasma glucose reflecting the PPP activity was very low in these healthy patients under all conditions and that fasting increases hepatic PPP activity, gluconeogenesis from glycerol, and glycerol metabolism through the TCA cycle prior to gluconeogenesis. TAG synthesis and secretion to the bloodstream was continuous under the fed plus glucose condition but transient under a fast. This study also demonstrated for the first time that a significant fraction of the backbones of TAGs derived from an oral glycerol load was metabolized through the TCA cycle prior to glyceroneogenesis in the liver of human subjects.

This is the first report to assess hepatic PPP in human subjects after oral administration of a gluconeogenic, stable isotope substrate. Typically ^{13}C-labeled glucose tracers have been used in isolated livers or hepatocytes to estimate PPP activity. For example, [1,2-$^{13}C_2$]glucose is converted to [2,3-$^{13}C_2$]lactate and unlabeled lactate via glycolysis but generates [3-$^{13}C_1$] lactate and unlabeled lactate after passage through the PPP. However, glucose tracers have limited utility *in vivo* for analysis of hepatic metabolism because glucose is potentially consumed by essentially all the organs of the body. Magnusson *et al.* (17) used radioactive tracers, [1-$^{14}C_1$]ribose and [2-$^{14}C_1$]glucose, and drugs, diflunisal and acetaminophen, to detect hepatic PPP activity in humans by analyzing glucuronides in urine. The use of radioactive tracers is a disadvantage because of safety and ethical concerns and the technical requirements for radiation containment. Furthermore, the drugs used to capture glucuronides may themselves alter PPP activity because the liver is the primary organ for detoxification of these probes. We analyzed glucose secreted from the liver receiving [U-$^{13}C_3$]glycerol and assumed that the liver is the dominant gluconeogenic organ in healthy humans. Glycerol is safe, and high doses (≥1 g/kg) of glycerol are commonly used for studies of exercise performance (18–20). In the current study, a much lower dose (50 mg/kg) of ^{13}C-labeled glycerol produced high quality spectra of plasma metabolites of interest. The major products of the PPP are NADPH and ribose. NADPH is a reducing agent, and ribose is essential for nucleotide synthesis. With this low dose of glycerol, we observed an increase in PPP activity during a fast that could be attributed to the increased need for NADPH for reduction of glutathione, a major antioxidant, because calorie restriction induces glutathione in the liver (21).

Excess nutrients in the liver are converted to TAGs, which are secreted into the circulation as very low density lipoproteins (22). The ^{13}C enrichment in the glycerol moiety provides an index of the final step of TAG synthesis, fatty acid esterification. TAG synthesis must be minimal under a fast, and for this rea-

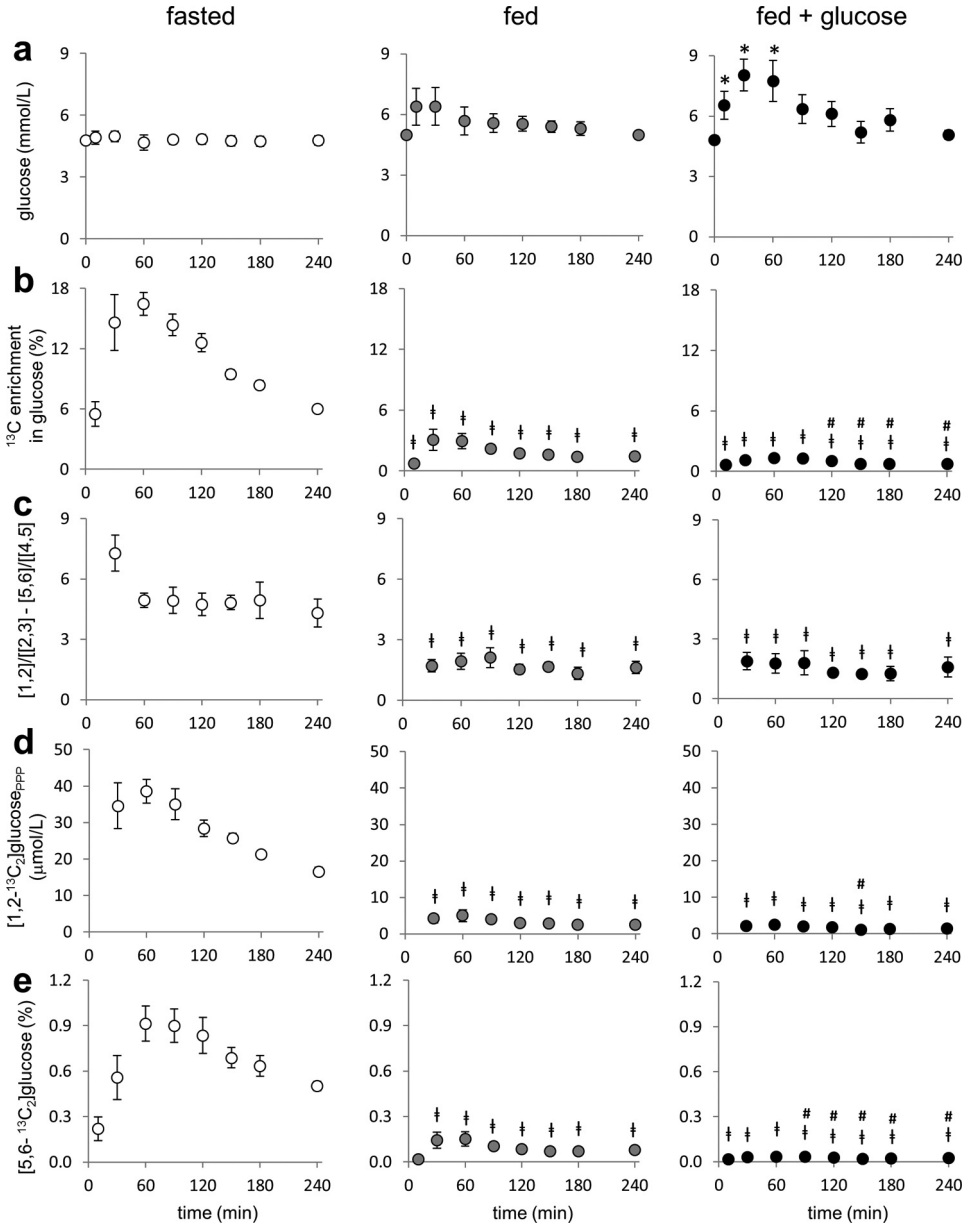

FIGURE 4. **Assessment of hepatic PPP and gluconeogenesis by analysis of plasma glucose from subjects receiving [U-$^{13}C_3$]glycerol.** *a*, plasma glucose remained the same under a fast and a fed condition but increased under a fed plus glucose condition. *b*, ^{13}C enrichment in glucose (reflecting gluconeogenesis from [U-$^{13}C_3$]glycerol) was higher under a fast condition than under a fed condition. The enrichment under a fed condition was slightly higher than a fed plus glucose condition at 120–240 min. The ^{13}C enrichment in glucose represents the sum of all glucose isotopomers with excess ^{13}C. *c*, as an index of hepatic PPP activity, the ratio difference between [1,2-$^{13}C_2$]/[2,3-$^{13}C_2$] and [5,6-$^{13}C_2$]/[4,5-$^{13}C_2$] in glucose was higher under a fast condition than under a fed condition, indicating that fasting induced the PPP activity. *d*, plasma [1,2-$^{13}C_2$]glucose produced through hepatic PPP was much higher under a fast condition than under a fed condition. *e*, the fraction of [5,6-$^{13}C_2$]glucose was greatest under a fast condition followed by a fed condition and a fed plus glucose condition. [5,6-$^{13}C_2$]Glucose was produced by [U-$^{13}C_3$]glycerol metabolism through the TCA cycle prior to gluconeogenesis. *[1,2]*, [1,2-$^{13}C_2$]glucose; *[2,3]*, [2,3-$^{13}C_2$]glucose, etc.; *[1,2-$^{13}C_2$]glucose$_{PPP}$*, [1,2-$^{13}C_2$]glucose produced through the PPP. *, $p < 0.05$ compared with $t = 0$ within each graph; ‡, $p < 0.05$ compared with the corresponding time point under a fasted state; #, $p < 0.05$ compared with the corresponding time point under a fed state ($n = 4–6$).

son the rapid incorporation of [U-$^{13}C_3$]glycerol into TAGs after a fast was not expected in the current study. The exogenous glycerol supply must trigger the esterification with abundant fatty acids after a fast. The appearance of newly produced TAGs did not necessarily lead a higher level of TAGs in plasma. Although [U-$^{13}C_3$]glycerol incorporation to TAGs was observed under all nutritional states, [TAG] increased only for a short period under the fed condition. This means either (i) the amount of newly synthesized TAGs from the liver was relatively small compared with total TAG pool in plasma or (ii) the clearance of TAGs by adipose tissue increased (23).

Because of the common route to triose pools from the TCA cycle, any double-labeled ^{13}C isotopomer detected in either glucose or the glycerol moiety in plasma serves as a biomarker for the anabolic function of hepatic mitochondria. It is important to detect this hepatic process because many liver diseases are considered to have defects in mitochondria biosynthetic pathways (24–26). [5,6-$^{13}C_2$]Glucose production, a marker for

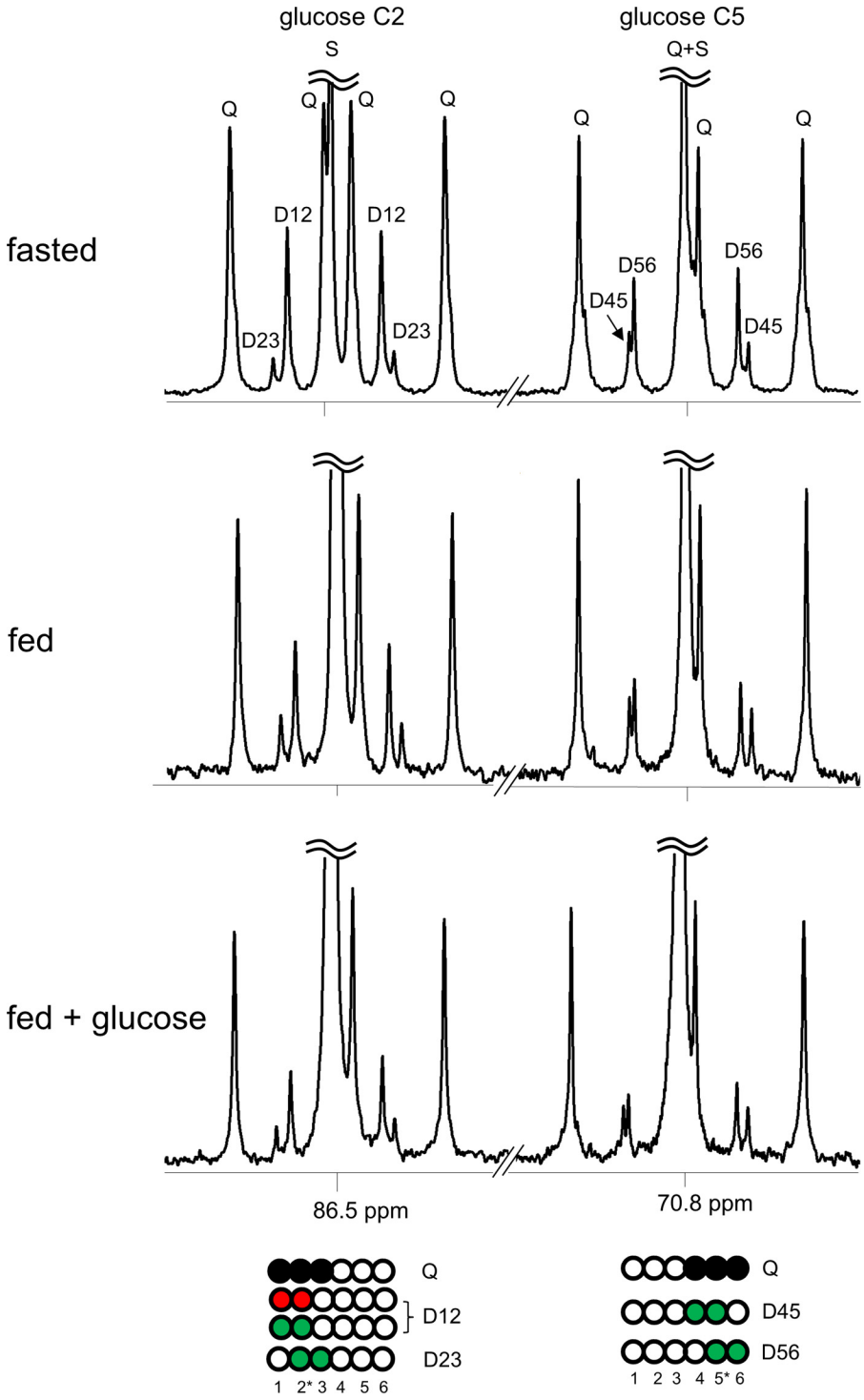

FIGURE 5. **^{13}C NMR spectra of plasma glucose reflect hepatic gluconeogenesis and PPP activity.** A subject ingested [U-$^{13}C_3$]glycerol under differing nutritional states, and blood was drawn at multiple times. Glucose was derivatized for ^{13}C NMR acquisition, and the spectra are from blood drawn at 180 min after [U-$^{13}C_3$]glycerol ingestion. Gluconeogenesis directly from [U-$^{13}C_3$]glycerol produced [1,2,3-$^{13}C_3$]- and [4,5,6-$^{13}C_3$]glucose. [U-$^{13}C_3$]Glycerol metabolism through the TCA cycle prior to gluconeogenesis produced double-labeled glucose ([1,2-$^{13}C_2$], [2,3-$^{13}C_2$], [5,6-$^{13}C_2$], and [4,5-$^{13}C_2$]). Hepatic PPP activity produced additional [1,2-$^{13}C_2$]glucose, which was greatest under a fast. The ratio difference between D12/D23 *versus* D56/D45 (*i.e.* [1,2-$^{13}C_2$]/[2,3-$^{13}C_2$] *versus* [5,6-$^{13}C_2$]/[4,5-$^{13}C_2$] in glucose) reflects hepatic PPP activity, which was sensitive to nutritional states. *D12*, doublet from coupling of C1 with C2; *D23*, doublet from coupling of C2 with C3; *Q*, doublet of doublets, or quartet, arising from coupling of C2 with both C1 and C3 or from coupling of C5 with both C4 and C6; *D45*, doublet from coupling of C4 with C5; D56, doublet from coupling of C5 with C6; *S*, singlet. *Open circles*, ^{12}C; *black circles*, ^{13}C; *green circles*, ^{13}C after metabolism through the TCA cycle; *red circles*, ^{13}C after metabolism through the PPP.

gluconeogenesis of [U-$^{13}C_3$]glycerol through the TCA cycle, was noticeably increased under the fasting but minimal under the fed plus glucose condition. The indirect contribution of [U-$^{13}C_3$]glycerol to TAGs through the TCA cycle demonstrated the same conclusion. In the current study, monitoring [5,6-$^{13}C_2$]glucose provides a lower limit for detection of

TABLE 1
^{13}C NMR analysis of plasma glucose from subjects receiving [U-$^{13}C_3$]glycerol under different nutritional states

	30 min	60 min	90 min	120 min	150 min	180 min	240 min
Glucose produced through the PPP (%)							
Fasted	0.70 ± 0.14	0.85 ± 0.08	0.74 ± 0.11	0.59 ± 0.05	0.55 ± 0.04	0.46 ± 0.03	0.35 ± 0.03
Fed	0.08 ± 0.03[a]	0.10 ± 0.03[a]	0.08 ± 0.02[a]	0.05 ± 0.01[a]	0.05 ± 0.01[a]	0.05 ± 0.01[a]	0.05 ± 0.01[a]
Fed + glucose	0.03 ± 0.01[a,b]	0.03 ± 0.01[a,b]	0.04 ± 0.01[a,b]	0.03 ± 0.00[a,b]	0.02 ± 0.00[a,b]	0.02 ± 0.01[a,b]	0.03 ± 0.01[a,b]
PPP/gluconeogenesis from [U-$^{13}C_3$]glycerol (%)[c]							
Fasted	4.7 ± 0.6	5.1 ± 0.3	5.1 ± 0.6	4.9 ± 0.6	5.9 ± 0.4	5.5 ± 0.4	5.8 ± 0.5
Fed	2.5 ± 0.3[a]	2.9 ± 0.4[a]	3.3 ± 0.5[a]	3.1 ± 0.4[a]	3.2 ± 0.2[a]	3.1 ± 0.5[a]	3.4 ± 0.4[a]
Fed +glucose	2.5 ± 0.4[a]	2.4 ± 0.3[a]	2.8 ± 0.4[a]	3.1 ± 0.4[a]	2.9 ± 0.2[a]	2.9 ± 0.6[a]	4.0 ± 0.7[a]
[1,2-$^{13}C_2$] / [2,3-$^{13}C_2$] in glucose							
Fasted	10.3 ± 1.1	8.2 ± 0.7	8.1 ± 0.8	8.3 ± 0.6	8.1 ± 0.5	8.5 ± 1.0	7.7 ± 0.8
Fed	4.2 ± 0.4[a]	4.2 ± 0.6[a]	4.2 ± 0.7[a]	3.7 ± 0.4[a]	3.6 ± 0.5[a]	3.2 ± 0.4[a]	3.6 ± 0.4[a]
Fed + glucose	3.8 ± 0.4[a]	3.7 ± 0.6[a]	3.5 ± 0.7[a]	2.9 ± 0.2[a]	2.7 ± 0.2[a]	2.8 ± 0.4[a]	3.2 ± 0.6[a]
[5,6-$^{13}C_2$] / [4,5-$^{13}C_2$] in glucose							
Fasted	3.0 ± 0.3	3.2 ± 0.4	3.2 ± 0.3	3.6 ± 0.4	3.2 ± 0.2	3.5 ± 0.2	3.4 ± 0.2
Fed	2.5 ± 0.2	2.2 ± 0.2	2.1 ± 0.3[a]	2.1 ± 0.3[a]	1.9 ± 0.3[a]	1.9 ± 0.2[a]	2.0 ± 0.2[a]
Fed + glucose	1.9 ± 0.1[a,b]	2.0 ± 0.2[a]	1.7 ± 0.1[a]	1.5 ± 0.1[a]	1.4 ± 0.1[a]	1.5 ± 0.1[a]	1.6 ± 0.2[a]

[a] $p < 0.05$ compared to the corresponding time point under a fasted state.
[b] $p < 0.05$ compared to the corresponding time point under a fed state.
[c] The percentage of [1,2-$^{13}C_2$]glucose produced through hepatic PPP out of all glucose isotopomers with excess ^{13}C produced through gluconeogenesis from [U-$^{13}C_3$]glycerol ($n = 5–6$).

[U-$^{13}C_3$]glycerol metabolism through the TCA cycle. [U-$^{13}C_3$]Glycerol could be metabolized to [U-$^{13}C_3$]pyruvate followed by carboxylation to [1,2,3-$^{13}C_3$]oxaloacetate. If this metabolite is directly converted to [U-$^{13}C_3$]PEP (without further metabolism in the TCA cycle), then the ^{13}C labeling in glucose would be indistinguishable from direct conversion of [U-$^{13}C_3$]glycerol to glucose.

In summary, key metabolic processes in the liver including the PPP, fatty acid esterification, gluconeogenesis, and glyceroneogenesis were monitored in human subjects after oral administration of [U-$^{13}C_3$]glycerol. These processes are highly relevant for understanding high impact liver diseases such as fatty liver disease, type 2 diabetes, and hepatotoxicity. Glucose overproduction from the TCA cycle is a key feature of hepatic insulin resistance observed in fatty liver disease or type 2 diabetes. As noted, PPP provides reducing equivalents for antioxidant defense, which is impaired in hepatotoxicity caused by drugs such as acetaminophen. For the first time, flux of glycerol into the TCA cycle prior to gluconeogenesis or glyceroneogenesis was demonstrated in human subjects. This is also the first use of a ^{13}C-enriched gluconeogenic substrate to detect hepatic PPP activity in humans. From the subject's perspective, the exam was readily accepted and quite simple. The [U-$^{13}C_3$]glycerol method described here could be valuable for detecting biomarkers of liver diseases and for monitoring progression of such diseases.

Experimental Procedures

Research Design—This study was approved by the Institutional Review Board at the University of Texas Southwestern Medical Center. Each participant provided written informed consent prior to participation. Six healthy volunteers (ages, 24–47 years; body mass index, 19–26 kg/m^2; 4 males and 2 females; 3 Caucasians and 3 Asians) were recruited for this study. They completed three visits for differing study conditions (*i.e.* fasted, fed, or fed plus glucose) with at least 2 months separating each visit. Subjects with any chronic illness or use of medication aside from occasional antihistamines, aspirin or nonsteroidal anti-inflammatory drugs were excluded. The order of the study conditions for each subject was random. All subjects had a meal at 6:30 p.m. and started fasting at 7:00 p.m. on the day prior to the study. At 8:00 a.m. on the study day after the overnight fast, subjects were admitted to the Advanced Imaging Research Center located on the North Campus of University of Texas Southwestern. An intravenous catheter was positioned in an antecubital vein, and blood (10 ml) was drawn for chemistry at baseline. For the fasted study group, subjects ingested 50 mg/kg body weight [U-$^{13}C_3$]glycerol (99%; Sigma) dissolved in water followed by a series of blood draws (30 ml each) at 10, 30, 60, 90, 120, 150, 180, and 240 min. For the fed study group, subjects ate a meal (680 calories; 18% protein, 28% fat, and 54% carbohydrates) at 8:30 a.m., and received [U-$^{13}C_3$]glycerol (50 mg/kg) 60 min after the meal, followed by the same series of blood draws. For the fed plus glucose study group, subjects had the same meal at 8:30 a.m., plus ingested a mixture of glucose (1 g/kg) and [U-$^{13}C_3$]glycerol (50 mg/kg) 60 min after the meal. Again, blood was drawn over the same time points.

Sample Processing for NMR Analysis—Plasma (3 ml) was transferred into a 20-ml glass vial containing a chloroform/methanol mixture (2:1, 12 ml). The mixture was stirred for at least 30 min and centrifuged at a low rpm for organic-aqueous layer separation. The bottom chloroform layer containing lipids was transferred to a new glass vial. Chloroform (8 ml) was added to the first vial, and the mixture was stirred to repeat the extraction. The bottom chloroform layer was transferred, combined with the first one, and evaporated under vacuum with a liquid nitrogen trap. The dried lipids were dissolved in deuterated chloroform ($CDCl_3$, 170 μl; Cambridge Isotopes, Andover, MA) for ^{13}C NMR acquisition. Plasma glucose was extracted, purified, and converted to monoacetone glucose as described previously (10).

NMR Spectroscopy—All NMR spectra were collected using a Varian Inova 14.1 T spectrometer (Agilent, Santa Clara, CA) equipped with a 3-mm broadband probe with the observe coil

tuned to ^{13}C (150 MHz). ^{13}C NMR spectra of lipids were collected using a 60° pulse, a sweep width of 36,765 Hz, 110,294 data points, and a 1.5-s acquisition time with 1.5-s interpulse delay at 25 °C. Proton decoupling was performed using a standard WALTZ-16 pulse sequence. The spectra were averaged ~23,000 scans requiring 20 h. The solvent ($CDCl_3$) resonance set to 77.2 ppm was used as reference. ^{13}C NMR spectra of monoacetone glucose derived from glucose were collected as described previously (10). All NMR spectra were analyzed using ACD/Labs NMR spectral analysis program (Advanced Chemistry Development, Inc., Toronto, Canada).

Pathway Considerations for [U-$^{13}C_3$]glycerol Contributing to TAGs—Metabolism of [U-$^{13}C_3$]glycerol directly to the backbones of TAGs will generate intact ^{13}C 3-units (^{13}C-^{13}C-^{13}C). In contrast, if [U-$^{13}C_3$]glycerol is first metabolized to pyruvate and the TCA cycle prior to glyceroneogenesis, double-labeled ([1,2-$^{13}C_2$] and [2,3-$^{13}C_2$]) and triple-labeled ([U-$^{13}C_3$]) glycerol moieties will appear in TAG pool (Fig. 1*a*). The details of metabolic processes through the TCA cycle are complicated (16), but the following, relatively simple routes show how double-labeled trioses are produced through the metabolism of [U-$^{13}C_3$]glycerol in the TCA cycle. The entry of [U-$^{13}C_3$] pyruvate to the TCA cycle through pyruvate carboxylase produces 4-carbon intermediate, [1,2,3-$^{13}C_3$]oxaloacetate first. Because oxaloacetate is in rapid exchange with a symmetric fumarate pool, [2,3,4-$^{13}C_3$]oxaloacetate is also produced (Fig. 6*a*). In contrast, the entry of [U-$^{13}C_3$]pyruvate through pyruvate dehydrogenase generates [U-$^{13}C_2$]acetyl-CoA, and its condensation with unlabeled oxaloacetate results in [4,5-$^{13}C_2$]citrate. This becomes [4,5-$^{13}C_2$]α-ketoglutarate and consequently [3,4-$^{13}C_2$]-succinyl-CoA through the "forward" turn of the TCA cycle, experiencing decarboxylation twice. Again a symmetric fumarate pool produces double-labeled (*i.e.* [1,2-$^{13}C_2$] or [3,4-$^{13}C_2$]) 4-carbon intermediates and consequently equal amounts of [1,2-$^{13}C_2$]oxaloacetate and [3,4-$^{13}C_2$] oxaloacetate (Fig. 6*b*). Thus, [1,2,3-$^{13}C_3$]-, [2,3,4-$^{13}C_3$]-, [1,2-$^{13}C_2$]-, and [3,4-$^{13}C_2$]oxaloacetate are produced shortly after the entry of [U-$^{13}C_3$]pyruvate to the TCA cycle. Other isotopomers are possible through the metabolic network involving the TCA cycle, but will not be discussed for simplicity. Oxaloacetate may exit the TCA cycle via PEP carboxykinase to yield PEP after decarboxylation of oxaloacetate C4. As the result, [U-$^{13}C_3$]-, [2,3-$^{13}C_2$]-, [1,2-$^{13}C_2$]-, and [3-$^{13}C_1$]PEP are produced from [1,2,3-$^{13}C_3$]-, [2,3,4-$^{13}C_3$]-, [1,2-$^{13}C_2$]-, and [3,4-$^{13}C_2$]oxaloacetate, respectively. These PEP isotopomers can be transferred to other trioses along glyceroneogenic or gluconeogenic processes. Among the trioses, triple- and single-labeled trioses are not considered further in the estimation of indirect contribution of [U-$^{13}C_3$]glycerol to TAGs. The triple-labeled triose cannot be distinguished from the "direct" contribution of [U-$^{13}C_3$]glycerol, and the single-labeled triose cannot be differentiated from natural abundance one. In the current study, the appearance of double-labeled ([1,2-$^{13}C_2$] or [2,3-$^{13}C_2$]) glycerol in TAGs reflects the "indirect" contribution from [U-$^{13}C_3$] glycerol through the TCA cycle. The presence of [U-$^{13}C_3$]-glycerol in TAGs largely reflects "direct" conversion of [U-^{13}C]glycerol but could also contain a small indirect contribution. We report the indirect contribution of [U-$^{13}C_3$]glycerol based on the appearance of double-labeled glycerol moiety of TAGs and the direct contribution based on the appearance of [U-$^{13}C_3$]glycerol moiety. This means that the indirect contribution may be underestimated, whereas the direct contribution of the orally administered glycerol may be slightly overestimated.

In the ^{13}C NMR spectra of lipids, the multiplets contributing to the glycerol moiety C2 resonance of TAGs at 69.1 ppm is informative about the direct *versus* indirect contribution (Fig. 3*a*). The doublet (D) reflects contributions from [1,2-$^{13}C_2$]- and [2,3-$^{13}C_2$]glycerol, whereas the triplet (T, actually a doublet of doublets) reflects the contribution from [U-$^{13}C_3$]glycerol only. The relative signal area of the triplet, 1:2:1, is due to degeneracy in ^{13}C-^{13}C coupling constants in the [U-$^{13}C_3$]glycerol moiety. The middle peak of the triplet overlaps with the singlet but can be estimated by adding the areas of two lateral peaks of the triplet. The indirect and direct contributions of [U-$^{13}C_3$]glycerol to TAGs are straight readout of multiplet areas of double-labeled and triple-labeled glycerol moieties, respectively.

Analysis of Glucose Isotopomers for the Assessment of Hepatic PPP Activity—After phosphorylation in the liver, [U-$^{13}C_3$] glycerol can be further converted to [U-$^{13}C_3$]dihydroxyacetone phosphate (DHAP) or [U-$^{13}C_3$]glyceraldehyde 3-phosphate (GA3P). Condensation of [U-$^{13}C_3$]DHAP and unlabeled GA3P produces [1,2,3-$^{13}C_3$]hexose, whereas [4,5,6-$^{13}C_3$]hexose would be produced by combining unlabeled DHAP and [U-$^{13}C_3$]GA3P (Fig. 1*a*). These are the major glucose isotopomers generated in liver after receiving oral [U-$^{13}C_3$]glycerol. [U-$^{13}C_6$]Glucose could also be formed by condensation of [U-$^{13}C_3$]DHAP and [U-$^{13}C_3$]GA3P. Analysis of hepatic PPP activity is based on the principle that the ^{13}C-labeling patterns in the "top" or "bottom" half of glucose carbons reflect the triose pool and that the relative concentrations of double-labeled trioses cannot be altered by transaldolase activity or incomplete equilibration at the level of triose phosphate isomerase (15). Transaldolase activity exchanges fructose 6-phosphate carbons 4–6 with GA3P carbons. Neither process breaks covalent bonds in the triose pool. As noted, [U-$^{13}C_3$]glycerol metabolism through the TCA cycle produces double-labeled ([2,3-$^{13}C_2$] and [1,2-$^{13}C_2$]) PEP, which are common precursors for DHAP and GA3P, and subsequently glucose carbons 1–3 and carbons 4–6 (Fig. 1*a*). In this situation, the ratio of [1,2-$^{13}C_2$]/[2,3-$^{13}C_2$] in glucose must equal the ratio of [5,6-$^{13}C_2$]/[4,5-$^{13}C_2$] if there is no PPP activity. However, flux of [1,2,3-$^{13}C_3$]glucose 6-phosphate through the PPP produces [1,2-$^{13}C_2$]fructose 6-phosphate, as described previously (15). This increases the ratio of [1,2-$^{13}C_2$]/[2,3-$^{13}C_2$] appearing in glucose. In contrast, the ^{13}C 3-unit (^{13}C-^{13}C-^{13}C) in [4,5,6-$^{13}C_3$]hexose remains the same if this passes through the PPP (Fig. 1*b*). In this case, PPP would not alter the ratio of [5,6-$^{13}C_2$]/[4,5-$^{13}C_2$] in glucose. Consequently the ratio difference between [1,2-$^{13}C_2$]/[2,3-$^{13}C_2$] and [5,6-$^{13}C_2$]/[4,5-$^{13}C_2$] in glucose is sensitive to the PPP activity.

Fig. 5 shows spectra of monoacetone glucose derived from plasma glucose of a subject receiving [U-$^{13}C_3$]glycerol under differing nutritional states, Hepatic PPP activity is estimated based on the analysis of the spectra. As an example with a spec-

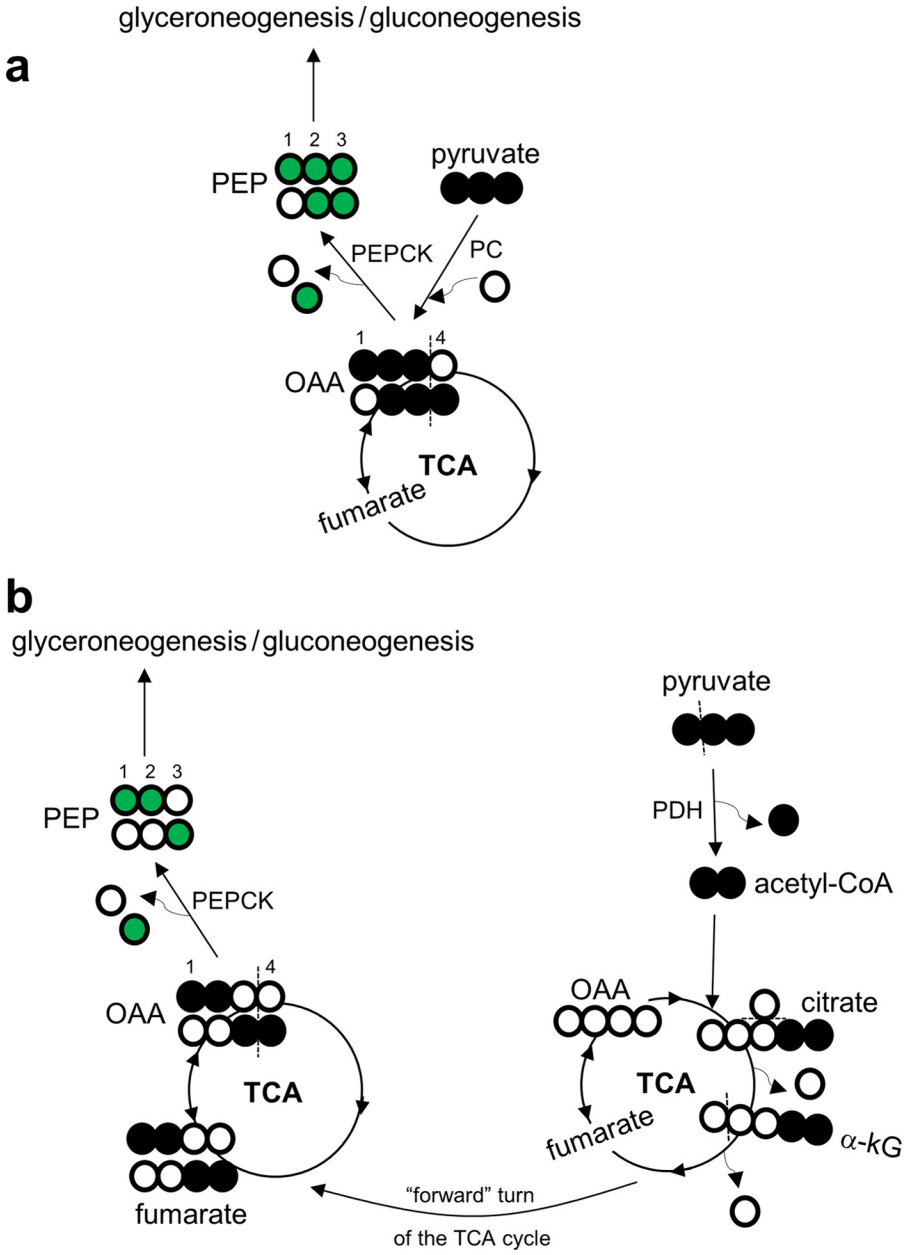

FIGURE 6. **Double-labeled trioses produced through the metabolism of [U-$^{13}C_3$]glycerol in the TCA cycle.** After phosphorylation, [U-$^{13}C_3$]glycerol may be further metabolized to [U-$^{13}C_3$]pyruvate entering the TCA cycle. *a*, the entry of [U-$^{13}C_3$]pyruvate through pyruvate carboxylase produces [1,2,3-$^{13}C_3$]oxaloacetate, which equilibrates with the symmetric fumarate pool, producing both [1,2,3-$^{13}C_3$]- and [2,3,4-$^{13}C_3$]oxaloacetate. These oxaloacetate isotopomers may exit the TCA cycle through PEP carboxykinase generating [U-$^{13}C_3$]PEP and [2,3-$^{13}C_2$]PEP. *b*, the entry of [U-$^{13}C_3$]pyruvate through pyruvate dehydrogenase generates [U-$^{13}C_2$]acetyl-CoA. The condensation of [U-$^{13}C_2$]acetyl-CoA and oxaloacetate produces [4,5-$^{13}C_2$]citrate and [4,5-$^{13}C_2$]α-ketoglutarate. After decarboxylation and experiencing a symmetric fumarate pool, [1,2,-$^{13}C_2$]- and [3,4-$^{13}C_2$]oxaloacetate are produced. These isotopomers become [1,2-$^{13}C_2$]PEP and [3-$^{13}C_1$]PEP through PEP carboxykinase. *Open circle*, ^{12}C; *black circle*, ^{13}C; *green circle*, ^{13}C after metabolism through the TCA cycle. *kG*, ketoglutarate; *OAA*, oxaloacetate; *PC*, pyruvate carboxylase; *PDH*, pyruvate dehydrogenase; *PEPCK*, phospho*enol*pyruvate carboxykinase.

trum in Fig. 5, the subject after an overnight fast had 4.5 mmol/liter glucose in plasma at 180 min of [U-$^{13}C_3$]glycerol ingestion, The fraction of plasma glucose derived from [U-$^{13}C_3$]glycerol was 9.1%, which was the sum of excess ^{13}C enrichments by all glucose isotopomers reflecting gluconeogenesis from [U-$^{13}C_3$]glycerol. The ^{13}C enrichment of each isotopomer was estimated using internal references (*i.e.* two methyl groups with natural abundance ^{13}C) of monoacetone glucose (27). The ratio [1,2-$^{13}C_2$]/[2,3-$^{13}C_2$] in glucose (*D12*/*D23* in Fig. 5) was 6.0, and the ratio [5,6-$^{13}C_2$]/[4,5-$^{13}C_2$] in glucose (*D56*/*D45*) was 3.0 under the fasting state. The area of D12 signal ($D12_{TOTAL}$) in the spectrum is the sum of [1,2-$^{13}C_2$]glucose signal arising from the PPP ($D12_{PPP}$) and [1,2-$^{13}C_2$]glucose arising through the TCA cycle ($D12_{TCA}$): $D12_{TOTAL} = D12_{PPP} + D12_{TCA}$. Because $D12_{TCA}/D23 = D56/D45$, $D12_{PPP} = D12_{TOTAL} - (D23 \times D56/D45)$. The calculated $D12_{PPP}$ in this case was 0.43% of plasma glucose, Thus the level of [1,2-$^{13}C_2$]$glucose_{PPP}$ was 19.4 μM (4500 μM $\times$ 0.0043). The relative PPP flux compared with gluconeogenesis form [U-$^{13}C_3$]glycerol was 4.7% (0.43/9.1).

Plasma Metabolite Assay—Plasma glucose was estimated using glucose oxidase (YSI 2300 glucose analyzer; GMI, Inc.). Fatty acids and TAGs in plasma were estimated using the Vitros

250 analyzers (Johnson & Johnson). Free glycerol in plasma was assayed using a commercial kit (Sigma).

Statistical Analysis—Data are expressed as means ± S.E. Comparisons between two groups were made using a Student's one-tailed *t* test, where $p < 0.05$ was considered significant.

Author Contributions—E. S. J. designed and supervised the experiments, acquired NMR spectra, analyzed the data, and wrote the manuscript. A. D. S. contributed to manuscript preparation. C. R. M. contributed to the conceptual approach and wrote the manuscript. All authors reviewed the results and approved the final version of the manuscript.

Acknowledgments—We thank Maghan Farrell, Maida Tai, Carol Parcel, Jeannie Baxter, Janet Jerrow, and Rebecca Murphy for technical support.

References

1. Li, S., Tan, H. Y., Wang, N., Zhang, Z. J., Lao, L., Wong, C. W., and Feng, Y. (2015) The role of oxidative stress and antioxidants in liver diseases. *Int. J. Mol. Sci.* **16,** 26087–26124
2. Takahashi, Y., Sugimoto, K., Inui, H., and Fukusato, T. (2015) Current pharmacological therapies for nonalcoholic fatty liver disease/nonalcoholic steatohepatitis. *World J. Gastroenterol.* **21,** 3777–3785
3. Neuschwander-Tetri, B. A., Loomba, R., Sanyal, A. J., Lavine, J. E., Van Natta, M. L., Abdelmalek, M. F., Chalasani, N., Dasarathy, S., Diehl, A. M., Hameed, B., Kowdley, K. V., McCullough, A., Terrault, N., Clark, J. M., Tonascia, J., Brunt, E. M., Kleiner, D. E., Doo, E, and NASH Clinical Research Network (2015) Farnesoid X nuclear receptor ligand obeticholic acid for non-cirrhotic, non-alcoholic steatohepatitis (FLINT): a multicentre, randomised, placebo-controlled trial. *Lancet* **385,** 956–965
4. Federico, A., Zulli, C., de Sio, I., Del Prete, A., Dallio, M., and Masarone, M., and Loguercio, C. (2014) Focus on emerging drugs for the treatment of patients with non-alcoholic fatty liver disease. *World J. Gastroenterol.* **20,** 16841–16857
5. Pawlyk, A. C., Giacomini, K. M., McKeon, C., Shuldiner, A. R., and Florez, J. C. (2014) Metformin pharmacogenomics: current status and future directions. *Diabetes* **63,** 2590–2599
6. Madiraju, A. K., Erion, D. M., Rahimi, Y., Zhang, X. M., Braddock, D. T., Albright, R. A., Prigaro, B. J., Wood, J. L., Bhanot, S., MacDonald, M. J., Jurczak, M. J., Camporez, J. P., Lee, H. Y., Cline, G. W., Samuel, V. T., Kibbey, R. G., and Shulman, G. I. (2014) Metformin suppresses gluconeogenesis by inhibiting mitochondrial glycerophosphate dehydrogenase. *Nature* **510,** 542–546
7. Sumida, Y., Nakajima, A., and Itoh, Y. (2014) Limitations of liver biopsy and non-invasive diagnostic tests for the diagnosis of nonalcoholic fatty liver disease/nonalcoholic steatohepatitis. *World J. Gastroenterol.* **20,** 475–485
8. Hellerstein, M. K., Neese, R. A., Linfoot, P., Christiansen, M., Turner, S., and Letscher, A. (1997) Hepatic gluconeogenic fluxes and glycogen turnover during fasting in humans. A stable isotope study. *J. Clin. Invest.* **100,** 1305–1319
9. Browning, J. D., Weis, B., Davis, J., Satapati, S., Merritt, M., Malloy, C. R., and Burgess, S. C. (2008) Alterations in hepatic glucose and energy metabolism as a result of calorie and carbohydrate restriction. *Hepatology* **48,** 1487–1496
10. Jin, E. S., Szuszkiewicz-Garcia, M., Browning, J. D., Baxter, J. D., Abate, N., and Malloy, C. R. (2015) Influence of liver triglycerides on suppression of glucose production by insulin in men. *J. Clin. Endocrinol. Metab.* **100,** 235–243
11. Diraison, F., Moulin, P., and Beylot, M. (2003) Contribution of hepatic *de novo* lipogenesis and reesterification of plasma non-esterified fatty acids to plasma triglyceride synthesis during non-alcoholic fatty liver disease. *Diabetes Metab.* **29,** 478–485
12. Bock, G., Schumann, W. C., Basu, R., Burgess, S. C., Yan, Z., Chandramouli, V., Rizza, R. A., and Landau, B. R. (2008) Evidence that processes other than gluconeogenesis may influence the ratio of deuterium on the fifth and third carbons of glucose: implications for the use of $^{2}H_{2}O$ to measure gluconeogenesis in humans. *Diabetes* **57,** 50–55
13. Rothman, D. L., Magnusson, I., Katz, L. D., Shulman, R. G., and Shulman, G. I. (1991) Quantitation of hepatic glycogenolysis and gluconeogenesis in fasting humans with ^{13}C NMR. *Science* **254,** 573–576
14. Magnusson, I., Rothman, D. L., Katz, L. D., Shulman, R. G., and Shulman, G. I. (1992) Increased rate of gluconeogenesis in type II diabetes mellitus. *J. Clin. Invest.* **90,** 1323–1327
15. Jin, E. S., Sherry, A. D., and Malloy, C. R. (2014) Interaction between the pentose phosphate pathway and gluconeogenesis from glycerol in the liver. *J. Biol. Chem.* **289,** 32593–32603
16. Jin, E. S., Sherry, A. D., and Malloy, C. R. (2013) Metabolism of glycerol, glucose, and lactate in the citric acid cycle prior to incorporation into hepatic acylglycerols. *J. Biol. Chem.* **288,** 14488–14496
17. Magnusson, I., Chandramouli, V., Schumann, W. C., Kumaran, K., Wahren, J., and Landau, B. R. (1988) Pentose pathway in human liver. *Proc. Natl. Acad. Sci. U.S.A.* **85,** 4682–4685
18. Massicotte, D., Scotto, A., Péronnet, F., M'Kaouar, H., Milot, M., and Lavoie, C. (2006) Metabolic fate of a large amount of ^{13}C-glycerol ingested during prolonged exercise. *Eur. J. Appl. Physiol.* **96,** 322–329
19. Van Rosendal, S. P., Strobel, N. A., Osborne, M. A., Fassett, R. G., and Coombes, J. S. (2012) Performance benefits of rehydration with intravenous fluid and oral glycerol. *Med. Sci. Sports Exerc.* **44,** 1780–1790
20. Goulet, E. D., Rousseau, S. F., Lamboley, C. R., Plante, G. E., and Dionne, I. J. (2008) Pre-exercise hyperhydration delays dehydration and improves endurance capacity during 2 h of cycling in a temperate climate. *J. Physiol. Anthropol.* **27,** 263–271
21. Ugochukwu, N. H., and Figgers, C. L. (2007) Dietary caloric restriction improves the redox status at the onset of diabetes in hepatocytes of streptozotocin-induced diabetic rats. *Chem. Biol. Interact.* **165,** 45–53
22. Ferré, P., and Foufelle, F. (2010) Hepatic steatosis: a role for de novo lipogenesis and the transcription factor SREBP-1c. *Diabetes Obes. Metab.* **12,** 83–92
23. Frayn, K. N. (2002) Adipose tissue as a buffer for daily lipid flux. *Diabetologia* **45,** 1201–1210
24. Auger, C., Alhasawi, A., Contavadoo, M., and Appanna, V. D. (2015) Dysfunctional mitochondrial bioenergetics and the pathogenesis of hepatic disorders. *Front. Cell Dev. Biol.* **3,** 40
25. Lee, W. S., and Sokol, R. J. (2007) Liver disease in mitochondrial disorders. *Semin. Liver Dis.* **27,** 259–273
26. Abdelmegeed, M. A., Banerjee, A., Yoo, S. H., Jang, S., Gonzalez, F. J., and Song, B. J. (2012) Critical role of cytochrome P450 2E1 (CYP2E1) in the development of high fat-induced non-alcoholic steatohepatitis. *J. Hepatol.* **57,** 860–866
27. Jin, E. S., Jones, J. G., Merritt, M., Burgess, S. C., Malloy, C. R., and Sherry, A. D. (2004) Glucose production, gluconeogenesis, and hepatic tricarboxylic acid cycle fluxes measured by nuclear magnetic resonance analysis of a single glucose derivative. *Anal. Biochem.* **327,** 149–155